4-28-2009

Adsorption of CO on Supported Gold Nanoparticle Catalysts: A Comparative Study

Heather Hartshorn
Trinity University

Christopher J. Pursell
Trinity University, cpursell@trinity.edu

Bert D. Chandler
Trinity University, bchandle@trinity.edu

Adsorption of CO on Supported Gold Nanoparticle Catalysts: A Comparative Study

Heather Hartshorn, Christopher J. Pursell,* and Bert D. Chandler*

Department of Chemistry, Trinity University, San Antonio, Texas 78212-7200

Received: March 20, 2009; Revised Manuscript Received: April 28, 2009

The adsorption of CO on three different gold nanoparticle catalysts supported on high surface area TiO_2 was studied using infrared transmission spectroscopy at room temperature and CO pressures typically used in CO oxidation reactions. The three, real-world catalysts were Au catalysts synthesized in our laboratory from thiol monolayer protected clusters (MPCs) and two commercial catalysts from the World Gold Council (WGC and AuTEK). Within experimental reproducibility, the adsorption data for the three catalysts are indistinguishable. While showing approximately Langmuir behavior, the adsorption data also show coverage dependence, as others have observed for many catalyst systems. Two approaches were used to fit the data, a two-site model and a variable binding constant model. The two-site Langmuir model yielded strong (36%) and weak (64%) binding constants of 2740 and 146 atm^{-1}, respectively. Alternatively, using a sliding-tangent Langmuir fit gave a variable binding constant of 2670−120 atm^{-1} at room temperature for coverage $\theta = 0-0.8$. The heat of adsorption was then extracted from the binding constants using a literature value for $-T\Delta S$. These values were determined as $\Delta H = -64$ and -56 kJ/mol for strong and weak binding according to the two-site model and $\Delta H = -63$ to -56 kJ/mol for coverage $\theta = 0-0.8$ for the variable binding constant model. These values agree well with literature values obtained (i) using supported catalysts under higher pressures and (ii) using model catalysts under higher pressures and ultrahigh vacuum conditions.

Introduction

Supported Au catalysts are now well-established as the most active low-temperature CO oxidation catalysts known.[1,2] Recent studies of gold and gold-based heterogeneous catalysts have extended the number of gold-catalyzed reactions to important reactions for industrial and synthetic chemists, including the water−gas shift reaction,[3] alcohol[4] and alkene[5] oxidations, hydrosilylation,[6,7] the selective hydrogenation of nitroaromatics,[8,9] and the production of commodity chemicals from biomass feedstocks.[10] Indeed, the field of Au catalysis may be described largely in a regime of exploratory science, with numerous research groups working to discover new reactions and investigate new potential applications for Au-based materials.

Despite the tremendous research activity in gold-catalyzed oxidation reactions, the origins of the catalytic activity are still under discussion. One complicating factor is the wide range of reported activities, particularly in the case of CO oxidation. A recent review indicates that CO oxidation activities can vary by orders of magnitude for catalysts prepared in different laboratories using similar preparation techniques.[2] However, to move from discovery-based science to deeper understanding, it is important to understand how catalysts differ and apply quantitative characterization techniques to compare catalysts prepared with different synthetic approaches.

To this end, carbon monoxide has long been used as a probe molecule for organometallic complexes, multimetallic metal clusters, and heterogeneous catalysts.[11−15] The CO stretching frequency (ν_{CO}) is remarkably sensitive to metal identity or electronic structure and can be used to rapidly evaluate the presence of metallic versus cationic surface metal atoms. It is also sensitive to adsorbate−adsorbate interactions. In the case of CO oxidation, the adsorption of CO is a likely fundamental step in the reaction mechanism and is, therefore, important to characterize in order to understand the catalysis.

Relative to other late transition metals, CO binding to the coinage metals is weak.[16] Only a few reports have been able to determine the number of available CO binding sites on supported gold catalysts, albeit at substantially subambient temperatures.[17,18] Consequently, there are relatively few infrared spectroscopic studies of CO adsorption on Au nanoparticles. Several studies have been performed on model catalysts under UHV conditions. Goodman's group examined CO adsorption on Au clusters deposited on TiO_2/Mo(110) at low pressures and temperatures.[19] They observed Langmuir-like adsorption on Au clusters with $d = 3.1$ nm, and isosteric plots yielded coverage-dependent heat of adsorption values. Behm's group also reported the adsorption of CO on Au clusters on TiO_2/Ru(0001) under UHV conditions (low temperature and pressure),[20] along with the more catalytically relevant conditions of $T = 30-120$ °C and $P_{CO} = 7.5-37.5$ Torr.[21] Using a version of Temkin's adsorption model, they determined coverage-dependent heat of adsorption values that varied slightly with cluster size.

Work examining Au nanoparticles on various substrates includes a study of CO adsorption on Au clusters deposited on FeO(111)/Pt(111). Lemire et al. reported size-dependent adsorption, which they attributed to the presence of highly uncoordinated gold atoms in very small particles.[22] Finally, Yim et al. examined low-temperature and -pressure CO adsorption on Au clusters deposited on highly oriented pyrolytic graphite (HOPG) and on Au(111) roughened by argon-ion bombardment.[23] They observed two TPD peaks with different heat of adsorption values, which they attributed to strong and weak binding. In particular, they noted the importance of low-coordinate steps and kinks in strongly binding CO.

A number of UHV studies on unsupported Au surfaces similarly provide important background for the present work.

* To whom correspondence should be addressed. E-mail: Bert.chandler@trinity.edu (B.D.C.), cpursell@trinity.edu (C.J.P.). Phone: (210) 999-7557 (B.D.C.), (210) 999-7381 (C.J.P.). Fax: (210) 999-7569 (B.D.C.), (C.J.P.).

10.1021/jp902553n CCC: $40.75
Published on Web 05/27/2009

Using a Au(110)−(1 × 2) surface,[24] Goodman's group observed heat of adsorption values that depended on coverage and attributed the interactions to low-coordinate Au sites. Koel's group examined CO adsorption on Au(211) and reported heat of adsorption values for step and terrace sites.[25] In particular, they observed low-coverage, strong non-Langmuirian binding on steps and higher-coverage, weaker Langmuirian binding on terraces.

Most of the infrared examinations of high surface area catalysts have involved single pressure measurements designed to characterize different catalysts. As such, there are relatively few pressure studies on high surface area catalysts, and few attempts have been made to determine the binding constant for CO adsorption. A recent study by Bianchi's group used infrared spectroscopy and relatively high pressures to measure the temperature dependence of isobaric CO adsorption on Au nanoparticle catalysts prepared via the deposition−precipitation method.[26] By employing a version of Temkin's adsorption model, Bianchi's group determined heat of adsorption values that were coverage-dependent. Beyond this, however, we are aware of no other determination of the equilibrium constant for CO binding on high surface area gold catalysts, and we are unaware of any direct isothermal measurements.

Consequently, we set out to use infrared spectroscopy to measure CO adsorption on high surface area catalysts at room temperature. Importantly, because these catalysts generally work near room temperature with approximately 1% CO, we sought to develop a methodology that investigates the materials under conditions as close to the catalytic working conditions as possible. We recently reported on a method for preparing highly active model Au catalysts from thiol monolayer protected clusters (MPCs) and showed that our new catalysts were somewhat more active, but comparable to traditionally prepared materials.[27] In the present study, we evaluate the fundamental step of CO adsorption on two commercial catalysts prepared via traditional means and compare them to the new bench scale catalyst. Our goals are to study CO adsorption as a fundamental step in CO oxidation catalysis and to compare CO adsorption on different catalysts to investigate its relative importance for influencing or predicting catalyst activity.

Experimental Section

Gold Nanoparticle Catalysts. The World Gold Council provided both the World Gold Council (WGC) and AuTEK catalysts. The WGC catalyst arrived as a powder and was used as received. The AuTEK catalyst arrived as ca. 5 × 10 mm pellets. This catalyst is prepared with an "eggshell" structure (Au predominantly deposited on the top few micrometers of the pellet), so the surface of individual pellets was scraped with a spatula. The scrapings were then ground to a powder in an agate mortar and pestle.

Details of the synthesis of the thiol monolayer protected catalyst (MPC) have been previously reported.[27,28] Briefly, Au nanoparticles were prepared in water using amine-terminated generation 5 polyamidoamine dendrimers (Dendritech). The nanoparticles were extracted into toluene as thiol monolayer protected clusters using decanethiol. After purification by multiple ethanol precipitations, the clusters were dissolved in methylene chloride and adsorbed onto the Degussa P-25 TiO_2 support with stirring. Reduction under H_2/N_2 at 300 °C for 16 h has been shown to remove the thiols and produce active CO oxidation catalysts.[27]

A complete structural and kinetic characterization of the MPC and WGC catalysts (transmission electron microscopy (TEM), X-ray photoelectron spectroscopy (XPS), diffuse reflectance infrared Fourier transform spectroscopy (DRIFTS), kinetics of CO oxidation catalysis) has been reported previously.[27] Importantly, the reduction treatment showed no observable changes in particle size for the WGC catalyst. Changes in Au particle size for the MPC catalyst were small and within the error of the TEM measurements; thus, this pretreatment does not appear to induce sintering for Au/TiO_2 catalysts. Accordingly, all catalysts underwent this reduction procedure prior to infrared spectroscopy measurements.

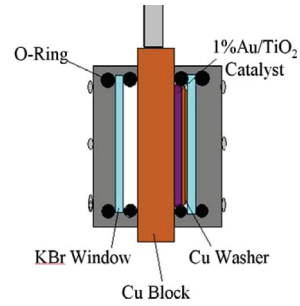

Figure 1. Cross section of the sample cell for infrared transmission spectroscopy of gold-supported catalysts. The Au/TiO_2 catalyst is pressed into a 30 × 30 Ti mesh and mounted inside the copper cell.

Infrared Spectroscopic Measurements. Catalyst samples for infrared analysis were prepared by pressing the Au/TiO_2 catalyst into a 30 × 30 Ti mesh (Unique Wire Weaving Co.). Most experiments were performed with approximately 20 mg of catalyst, but other masses between 15 and 34 mg were also used. The resulting mesh-supported pellet was placed in a tube furnace and heated overnight at 150 °C. After cooling, the mesh-supported pellet was mounted into a home-built copper cell and vacuum chamber; see Figure 1. This sample cell has a gas-phase optical path length of 1 cm. The entire vacuum chamber was placed in the sample compartment of a Nicolet Magna 550 FTIR spectrometer and evacuated to a pressure of <1 mTorr for 15 min. All measurements were made at an ambient temperature of 297 K. All spectra were referenced to a background spectrum of the Au/TiO_2 pellet under vacuum prior to the addition of CO. Transmission spectra consisted of 100 scans collected with 8 cm^{-1} resolution (spectral data spacing = 4 cm^{-1}) and were reported in absorbance units.

The gas handling system consisted of a mechanical and diffusion pump, a glass line with stainless steel transfer lines to the sample apparatus, and a Baratron pressure gauge (P = 0−10 Torr). A liquid nitrogen trap was used to trap out any impurities from the CO tank (UHP grade, from Air Products). The entire gas handling system was rinsed with CO three times before exposing the sample. After a background spectrum was collected, the sample was exposed to a low pressure of CO and the surface was allowed to equilibrate for 5−10 min. An infrared spectrum was recorded, and the pressure in the cell was slowly increased to the next pressure. After an experiment was completed, the sample was evacuated and the experiment repeated for a total of two or three adsorption isotherm measurements on a single catalyst sample in a single day.

Results

Three Au/TiO_2 catalysts (WGC, AuTEK, and MPC) were characterized by CO adsorption at room temperature using infrared transmission spectroscopy. Figure 2 shows the infrared spectra for a typical adsorption experiment for CO pressure from 0 to 10 Torr, in this case, using the World Gold Council (WGC) catalyst (34 mg pellet of 1% Au on TiO_2). Numerous control

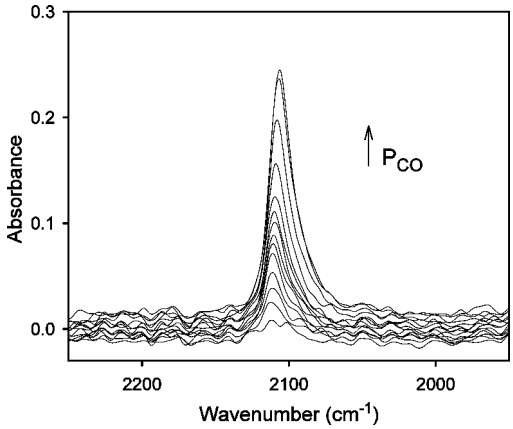

Figure 2. Infrared transmission spectra of CO adsorbed on the Au nanoparticle catalyst at room temperature (1% Au on TiO_2, WGC catalyst, 34 mg pellet). CO pressure was increased from 0 to 10 Torr. Integrated peak area represents the CO coverage at each pressure. The CO peak shows a red shift with increasing coverage.

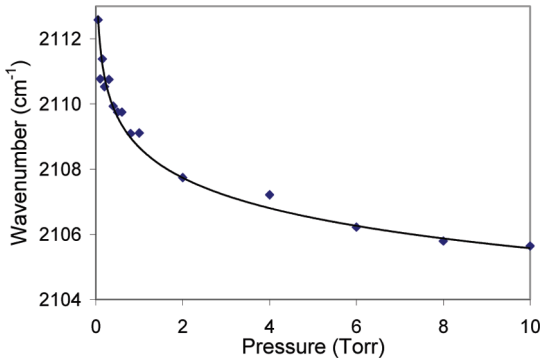

Figure 3. Infrared CO peak position showing a red shift as CO pressure increases. The smooth curve shown is to simply guide the eye.

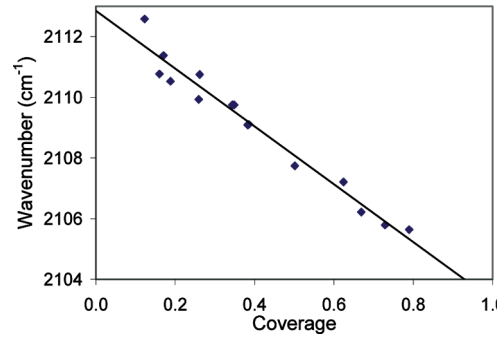

Figure 4. Infrared CO peak position showing a red shift with coverage. Coverage was determined from a Langmuir fit of the integrated peak area at higher CO pressures (see text and Figure 8). The line is a fit to the data, showing an approximately linear relationship.

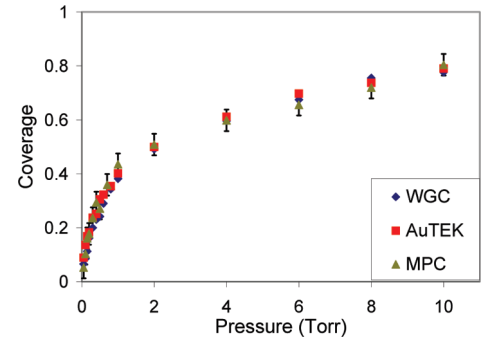

Figure 5. Langmuir isotherm plot for the three Au nanoparticle catalysts at room temperature. Coverage was determined from a Langmuir fit of the data at higher pressures (see text and Figure 8). Each point is the average of two to five individual experiments. Error bars representing one standard deviation are included for the MPC data. Within experimental reproducibility, all three catalysts exhibit similar coverage dependence.

experiments showed that the general features of the spectra were independent of the mass of catalyst used (only the peak area and maximum peak height changed). Additionally, the MPC and AuTEK catalysts had essentially the same spectra as those of the WGC catalyst, so plots similar to Figure 2 are omitted for brevity.

The infrared peak slightly above 2100 cm^{-1} is attributed to CO adsorption on Au; no adsorption on TiO_2 was observed at this temperature.[29] The peak position shows a moderate red shift from 2113 to 2106 cm^{-1} as the CO pressure increases, shown in Figure 3. The data also suggest that some of the CO adsorption sites remain open at 10 Torr, as there is a continued red shift in the CO stretching frequency at the high end of this pressure regime. All three gold catalysts exhibited very similar infrared spectra and red shifts, so only the data from the WGC catalyst are presented. This shift is consistent with previously published results for CO adsorption on gold.[19,22−25,30−34] The bonding between CO and Au is thought to occur through a combination of σ and π interactions.[34] Briefly, the 5σ bonding HOMO on CO donates into the metal s and d orbitals, stabilizing the HOMO and strengthening the CO bond. At the same time, the $2\pi^*$ antibonding LUMOs withdraw some electron density from the metal d orbitals, weakening the CO bond. Increasing CO coverage leads to an increase in electron density at the metal surface, which decreases the extent of 5σ donations from CO to Au. This, in turn, leads to a reduction in the stabilization of the 5σ bonding orbital, which leads to a slightly weaker CO bond and the observed red shift in the CO vibrational peak position.[34]

The infrared data can be interpreted in terms of surface coverage (described in detail below) and are plotted in Figure 4. Extrapolation of this plot to $\theta = 1$ yields a full-coverage CO stretching frequency of 2103.5 cm^{-1}, in excellent agreement with measurements on model UHV systems[19,22−25] and higher-pressure studies with other supported Au catalysts.[26]

The integrated peak area (S) was used to quantify the CO adsorption. The S values for individual IR spectra were converted to CO coverage (θ) by normalizing to the maximum integrated peak area (S_{max}) for that particular isotherm adsorption experiment (vide infra). In this normalization, where $\theta = S/S_{max}$, we examine only the coverage of CO binding sites and not necessarily the total coverage of the nanoparticle surface. The maximum peak area was determined from a Langmuir plot of the high-pressure data, as described below.

Figure 5 is a plot of coverage as a function of CO pressure for the three gold catalysts and shows that all three catalysts display very similar Langmuir-like behavior. Numerous control experiments using all the catalysts were performed, including experiments with differing pellet masses. In all cases, the normalized adsorption data showed essentially this same general behavior; hence, in Figure 5, we have presented averaged data from two to five individual isotherm experiments on each catalyst. Goodman's group also observed Langmuir-like behavior for the adsorption of CO on Au clusters deposited on TiO_2/Mo(110).[19] Their cluster size ($d = 3.1$ nm) is very similar to the particle size of the catalysts of this study.

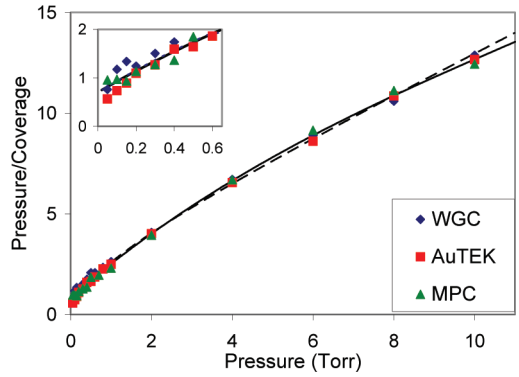

Figure 6. Room-temperature adsorption data for the three Au nanoparticle catalysts plotted over the entire pressure range in a linear form of the Langmuir equation. The data show a slight deviation from ideal Langmuir behavior over the large pressure range. A smooth, polynomial curve fit (solid line) has, therefore, been used to determine the binding constant as a function of coverage. Alternatively, the dashed line is a two-site model fit (see text).

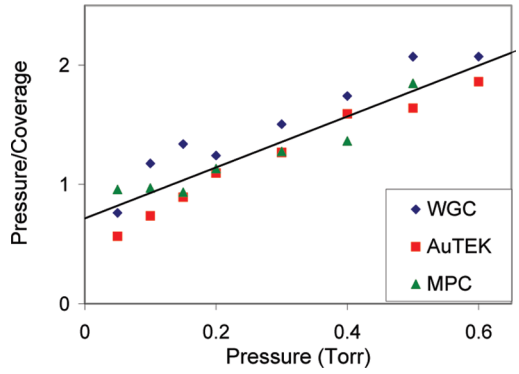

Figure 7. Lower-pressure adsorption data plotted in a linear form of the Langmuir equation. Within experimental reproducibility, the three catalysts have similar coverage dependence. The line is a fit of all data over this pressure range, demonstrating near-ideal Langmuir behavior.

The integrated infrared peak areas were, therefore, described using the following linear form of the Langmuir isotherm expression

$$\frac{P}{S} = \frac{1}{KS_{max}} + \frac{P}{S_{max}} \quad (1)$$

where P is the CO pressure in Torr, S is the CO integrated infrared peak area, S_{max} is the maximum peak area, and K is the equilibrium constant for CO binding to the Au nanoparticle surface.

Figure 6 shows the adsorption data plotted according to the linear form of the Langmuir expression given in eq 1. The data are not as linear as one might expect, and the solid curve included in the figure is a polynomial fit. This indicates that the adsorption process is more complicated than that of a single-site adsorption model (the Langmuir isotherm carries an implicit assumption that all of the adsorption sites are equivalent). The data in Figure 6 can be split into two regions under low and high CO pressures, shown in Figures 7 and 8, respectively. For the lower CO pressure range (ca. <1 Torr), the CO adsorption data show near-Langmuir behavior and, within experimental scatter of the data, the three catalysts are essentially equivalent.

The data exhibit very good Langmuir behavior over the higher CO pressure range (ca. 4−10 Torr). CO surface coverage, $\theta = S/S_{max}$, was defined using S_{max} determined from the high CO pressure fit of eq 1, as shown in Figure 8. The high-pressure data are closest to $\theta = 1$, which minimizes the error in the S_{max} value (determined from the slope of the line in Figure 8), giving what should be a reasonably precise value for S_{max}. The value for S_{max} was subsequently used to normalize the infrared peak area data, converting the individual peak areas to CO coverages.

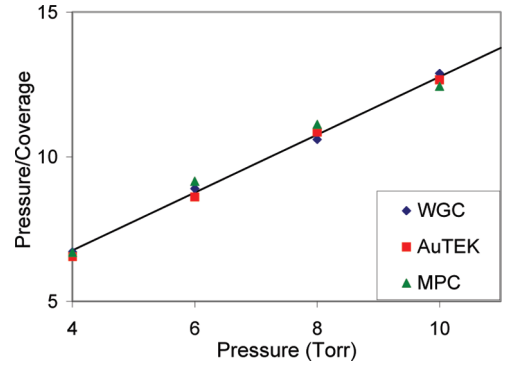

Figure 8. Higher-pressure adsorption data plotted in a linear form of the Langmuir equation. The line is a fit to all the data and has been used to convert the integrated infrared peak areas to coverage according to eq 1 (see text).

Figures 6−8 suggest that the adsorption data are best described by having a range of equilibrium constants (and, therefore, heats of adsorption) rather than a single binding constant. Coverage-dependent heat of adsorption is a well-known phenomenon and has been observed for a number of metal−adsorbate systems.[35−39] Several approaches can be used to describe the observed variation in K and ΔH with coverage; we employed two straightforward treatments.

The first approach invokes a two-site model involving collections of strong and weak binding sites. Accordingly, the integrated infrared peak area is a measure of the total coverage of all CO binding sites (not all gold surface sites). At low CO pressures, the adsorption would be to the strong binding sites, as per Figure 7, whereas at high pressures, adsorption is to the weak sites, as per Figure 8. Thus, the observed variation with pressure of the binding constant can then be described as a net binding constant that arises from the relative population and availability of these two sites. The adsorption data can, therefore, be expressed by the following two-site Langmuir model

$$\frac{S}{S_{max}} = \frac{f_s K_s P}{(1 + K_s P)} + \frac{f_w K_w P}{(1 + K_w P)} \quad (2)$$

where f_s and f_w are the fraction of strong and weak binding sites ($f_s + f_w = 1$) and K_s and K_w are the corresponding binding constants, respectively. Using SigmaPlot to fit the data to eq 2 yielded $K_s = 2740$ atm^{-1} (36% of the sites) and $K_w = 146$ atm^{-1} (64%). This fit is displayed in Figure 6 by the dashed curve through the data.

The second approach for accommodating the variation of K and ΔH is to analyze the data only over very small pressure (i.e. coverage) ranges, where the values of K and ΔH change only slightly. This can be done with a sliding-tangent fit to the Langmuir model shown in Figure 6. The data are fit to a polynomial function, and the derivative of that polynomial is calculated at discrete pressures to determine the slope of the curve ($1/S_{max}$) at that particular pressure. Using the determined slope and the point at which it was calculated, we calculate the intercept of the line tangent to the curve ($1/KS_{max}$) and use it to

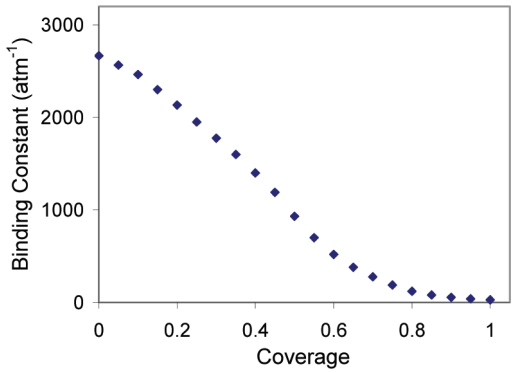

Figure 9. Binding constant for CO adsorption on Au nanoparticle catalysts at room temperature. The binding constant was determined according to eq 1 and the smooth curve in Figure 6. This analysis yields values of ΔG for CO adsorption that varies from −20 to −8 kJ/mol for low to high coverage, respectively. Since data were not collected for coverages above 0.8, the binding constants above 0.8 are an extrapolation of the fit.

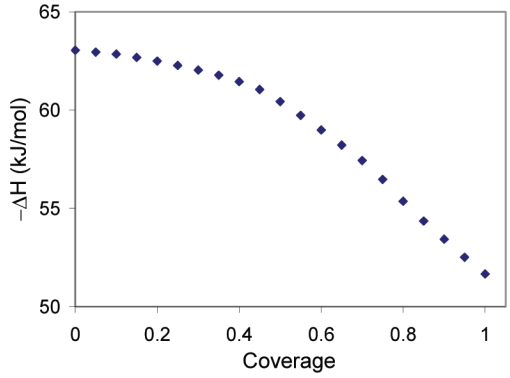

Figure 10. Enthalpy for CO adsorption on the three Au catalysts as a function of coverage. These values were determined from the binding constants at room temperature (see Figure 9) and a literature value for the entropy contribution, $T\Delta S = -44$ kJ/mol (see text).

extract the value of K at that particular pressure (i.e., coverage), or K = slope/intercept of eq 1.

When we use this model, the binding constant for CO on Au/TiO_2 catalysts varies from 2670 to 120 atm^{-1} at room temperature for $\theta = 0-0.8$, as shown in Figure 9. Since data were collected only to $\theta = 0.8$, we have extrapolated out to $\theta = 1$, where $K = 27$ atm^{-1}. Not surprisingly, the low- and high-coverage binding constant values agree with the two-site model's strong and weak binding constants.

From these K values, ΔG at room temperature (ca. 297 K) was determined as −20 and −12 kJ/mol for strong and weak binding sites, respectively, or as −20 to −8 kJ/mol over the range of $\theta = 0-0.8$. When we used these ΔG values and a $T\Delta S$ entropy contribution of −44 kJ/mol,[40] the ΔH of adsorption was determined to vary from −63 to −52 kJ/mol, as shown in Figure 10, or as −64 and −56 kJ/mol for strong and weak binding sites, respectively. To the best of our knowledge, this is the first time K values have been reported for the adsorption of CO on actual Au catalysts under pressures comparable to those typically used in catalytic test reactions. As shown in Table 1 and discussed further below, these heat of adsorption values agree very well with previous determinations at higher pressures and on model systems.

Discussion

The working state of any catalyst is of fundamental interest and importance, so examining catalysts under conditions as near as possible to the working conditions is highly desirable. The weak binding of CO to Au nanoparticles has made examination of this important interaction difficult, so most quantitative studies have been carried out with low surface area model catalysts under UHV conditions.[19,21,22,25] Studies with high surface area catalysts have been performed at much higher pressures,[26,41] where CO induced reconstruction of the Au nanoparticles was observed.[41] CO oxidation catalysts are typically tested at or near ambient pressure, nominally using 1% CO (7−8 Torr) and between 0.5 and 20% O_2.[2] To our knowledge, the present study is the first to examine CO binding on high surface area supported Au catalysts under conditions similar to those of working catalysts.

The real-world catalysts examined in this study include bench (WGC) and industrial-scale (AuTEK) catalysts prepared by traditional methods as well as a catalyst prepared from thiol-stabilized monolayer-protected clusters (MPC). The similarity in CO adsorption properties of the three catalysts is striking. Figure 5 shows that, within very reasonable errors, the three catalysts show essentially the same CO adsorption behavior. This is remarkable considering that the catalysts were prepared in three different laboratories, using vastly different preparation methods and production scales. It is even more surprising, in the context of the history of Au catalysis, where lab-to-lab reproducibility has only recently become common.[2] Given the small differences in the CO adsorption properties of the three catalysts, CO binding and activation are probably not primary factors in differentiating the activity of these catalysts.

Determination of K and ΔH. To the best of our knowledge, binding constants for the adsorption of CO on gold nanoparticle catalysts have not been reported in the literature.[1] Several groups have reported isobaric heat of adsorption measurements on Au nanoparticles, in which CO coverage was varied by changing the sample temperature (vida infra). These measurements have generally been made with model catalysts under UHV conditions or with high surface area catalysts using higher pressures. Our study is distinguished from these because we have made isothermal CO adsorption measurements on a variety of high surface area catalysts using pressures typically used in catalytic testing. This allows us to directly evaluate the equilibrium constant and extract the heat of adsorption to compare with literature measurements.

As shown in Figures 5−8, the three catalysts exhibit very similar near-Langmuir behavior. The slight deviation indicates that the adsorption process is more complicated than that of the single-site Langmuir adsorption model. However, without abandoning the simplicity of the Langmuir model, the data can be fit to modified expressions to determine experimental binding constants. The first approach is a two-site model, given by eq 2. As the dashed line through the data in Figure 6 shows, this simple model accurately represents the data. This model gives rise to two binding constants, $K = 2740$ and 146 atm^{-1}. It also provides an opportunity to estimate the relative number of strong (36%) and weak (64%) CO binding sites. Although this model may be an oversimplification, there are a number of literature reports describing two different CO adsorption regimes on model gold catalysts.[24,25,42]

Alternately, a Langmuir model with a coverage-dependent binding constant (and therefore binding energy) can be used to explain the differences in CO binding energy at low and high coverage. The fitting is accomplished using a sliding-tangent Langmuir expression, which also does a good job of describing the experimental data (the solid line through the data in Figure 6 nearly overlaps the two-site model fit). This model yields a

TABLE 1: Heat of Adsorption for CO on Au Catalysts and Surfaces

material	data analysis[a]	$-\Delta H_{str}$[b] (kJ/mol)	$-\Delta H_{wk}$[c] (kJ/mol)	P (Torr)	T (K)	θ	ref
Au/TiO_2	2-site Langmuir	64	56	$10^{-2}-10$	293	0–0.8	this work
Au/TiO_2	sliding tangent	63	56	$10^{-2}-10$	293	0–0.8	this work
Au/TiO_2	Temkin	74	47	8−150	125−400	0–1	26
2 nm $Au/TiO_2/Ru(0001)$	Temkin	74	40	8−40	303−493	0.3–0.7	21
3 nm $Au/TiO_2/Ru(0001)$	Temkin	66	42	8−40	303−493	0.3–0.7	21
4 nm $Au/TiO_2/Ru(0001)$	Temkin	62	44	8−40	303−493	0.3–0.7	21
1.8 nm $Au/TiO_2/Mo(111)$	C−C	69	63	$10^{-8}-10^{-2}$	130–220		19
2.5 nm $Au/TiO_2/Mo(111)$	C−C	76.2	60.7	$10^{-8}-10^{-2}$	130–220		19
3.1 nm $Au/TiO_2/Mo(111)$	C−C	52.3	27.2	$10^{-8}-10^{-2}$	130−220	0.05–0.9	19
$Au(110)-(1 \times 2)$	C−C	45.6	32.6	$10^{-8}-10^{-4}$	100−250	0–0.3	24
$Au/TiO_2/Ru(0001)$	TPD	65	53				20
Au(211) steps	TPD	50					25
Au(211) terraces	TPD	38	27				25
roughened Au(111)	TPD	54	44				23
Au/HOPG	TPD	51	39				23

[a] Data based on infrared spectroscopy or temperature-programmed desorption (TPD) measurements. C−C is a Clausius−Clapeyeron treatment of infrared adsorption data. [b] Heat of adsorption for strong CO binding sites (upper range of coverage-dependent heat of adsorption). [c] Heat of adsorption for weak CO binding sites (lower range of coverage-dependent heat of adsorption).

range of binding constants that gradually decrease from $K = 2670$ atm^{-1} at low coverage to $K = 120$ atm^{-1} at the highest coverage (ca. $\theta = 0.8$ at 10 Torr); see Figure 9. This model is consistent with literature reports of coverage-dependent binding energies, even when particle sizes are varied under controlled UHV conditions.[21,26]

We are unaware of other researchers using a sliding-tangent Langmuir expression to evaluate adsorption data on gold catalysts. The values extracted from this model are consistent with the more traditional two-site model as well as with literature reports (vida infra). The two models are slightly different ways of interpreting the data and yield essentially the same low- and high-coverage binding constants. Although the two-site model is likely to be an oversimplification, it does provide some information regarding the range of binding constants and the relative number of strong and weak binding sites.

The sliding-tangent model, on the other hand, more accurately reflects the complexity of a supported catalyst, which has a range of particle sizes and interactions with the irregular support. It is a simple and straightforward model that allows the binding constant to vary smoothly with coverage. Because the data are fit to an arbitrary fitting function and changes in the slope of this function with pressure are evaluated, the sliding-tangent model does not rely on assumptions regarding the nature of the interaction and does not extensively use fitting parameters.

Our approaches can be compared with the more complicated Temkin isotherm analysis utilized by Bianchi[26] and Behm.[21] In that model, the binding energy (or heat of adsorption) is assumed to vary linearly from a low coverage (E_0 at $\theta = 0$) to a high coverage value (E_1 at $\theta = 1$). The adsorption coefficients (K_0 and K_1, which are similar to binding constants) are determined using a statistical thermodynamics expression. Theoretical curves are then generated, and the E_0 and E_1 values (and, therefore, the K_0 and K_1 values) are adjusted until a good fit to the pressure-dependent coverage data at various temperatures is achieved. Although the Temkin analysis reproduces the adsorption data fairly well, it is rather complicated, assumes that the energy of adsorption varies linearly with coverage, and requires adsorption data at numerous temperatures.

Comparison to Literature Values. Table 1 is a compilation of the heat of adsorption values extracted from our measurements alongside previous measurements on other systems. It also includes some of the important experimental parameters. Only Bianchi's group has reported detailed CO adsorption measurements on high surface area Au/TiO_2 catalysts;[26] all of the other measurements are on single-crystal model systems. Bianchi's group used pressures of 8−150 Torr and subsequently discovered that the higher CO pressures induced some sort of reconstruction of the Au nanoparticles.[41] Typical reaction conditions are at 8 Torr or lower, so their measurements are at the upper boundary of those used in practice. Behm and coworkers used a slightly lower high-pressure range and were able to measure CO adsorption on different sized Au particles.[21] Goodman's group has also reported size-dependent CO adsorption, but under more typical UHV conditions. Our measurements on high surface area catalysts nicely fit in the gap between Goodman's, Behm's, and Bianchi's measurements.

Table 1 shows that our data fall well within the range of previous measurements. Our coverage-dependent ΔH values are bounded by Bianchi's measurements on similar materials and are very similar to both Behm and Goodman's measurements. This indicates that, at least for CO adsorption measurements on this system, the pressure and material gaps are not significant issues. The only real difference between our values and those reported by others is the range between the high and low coverage values. Our range is about 10 kJ/mol (which is similar to some of Goodman's ranges), whereas others typically report a range of 20 kJ/mol or more.

Koel's values are obtained from TPD measurements and, therefore, do not provide the same sort of coverage-dependence information.[25] They are, however, an important benchmark because they provide data for adsorption on the well-defined Au(211) surface.[25] Our strong binding sites (as our Bianchi's, Goodman's and Behm's) are more exothermic than Koel's measurements on Au(211) surfaces. This suggests that more highly uncoordinated Au corner and edge atoms are responsible for the strong CO binding, as others have concluded.[2] The lower range of our data approaches Koel's values, so surface arrangements resembling Au(211) surfaces may be involved in the weaker binding sites.

Implications for CO Oxidation Catalysis. Evaluating the current results based on previous CO oxidation studies with these catalysts and the context of the body of catalysis literature may also shed some light onto the important factors for the high activity of Au/TiO_2 catalysts. We recently reported an in-depth study of the preparation of the MPC catalyst as well as CO oxidation kinetics for both the WGC and MPC catalysts.[27] XPS and elemental analysis showed no residual sulfur on the MPC

catalyst after our activation protocol. Indirect measurements (IR, XPS, and TEM studies) were essentially identical for the WGC and MPC catalysts and showed no substantial differences between the two catalysts. Within very good experimental errors, the two catalysts have the same Arrhenius apparent activation energy and nearly identical reaction orders in both O_2 and CO. The only measurable difference between the two catalysts is the slightly higher activity of the MPC catalyst (ca. 40% faster rates per total Au), which was attributed to the preparation of a greater number of active sites when the preformed nanoparticles were used as catalyst precursors.

Three important conclusions regarding the reaction mechanism on working catalysts can be drawn from the current data: (i) the CO binding sites are likely to be under-coordinated corner and edge atoms (vide supra), (ii) these binding sites are not saturated with CO under typical reaction conditions, and (iii) oxygen, which binds much more weakly to Au than does CO (vida infra), can effectively compete with CO for low-coordination Au atoms. The directly observable red shift in CO stretching frequency (Figures 2−4) and the normalized peak area data (Figures 5 and 6) show that the catalysts are not saturated with CO under catalysis conditions (nominally 7−8 Torr). The important conclusion from this data is that, even at extremely low conversions (<1%) during catalysis, a substantial fraction of the CO adsorption sites (roughly 25%, see Figure 5) remain unoccupied.[43]In terms of a reaction mechanism, the presence of free CO binding sites means that CO desorption, which is inherently an endothermic process, is not required to open up a site for oxygen coordination. With more traditional Pt and Pd catalysts, CO binds too strongly and essentially covers all of the surface atoms, leaving few, if any, available sites for O_2 binding and activation.[44]

Our data probe the energetics of the interaction between CO and the Au surface and provide insight into the fraction of open CO binding sites; however, the data are only semiquantitative. We cannot evaluate the total number of CO binding sites, and it is important to clarify that these measurements are not equivalent to a chemisorption experiment. The data provide no direct information regarding the total number of CO binding sites, and it cannot be inferred that three-quarters of the total surface is covered by CO at 8 Torr. Our data only indicate that roughly 25% of the CO binding sites are available. Since these are likely to be under-coordinated corner and edge atoms, this is likely to be a small fraction of the total Au surface atoms.

Indeed, CO chemisorption values for supported Au catalysts have been notoriously difficult to measure, and researchers have often resorted to indirect methods to evaluate the number of active sites. For example, Oxford and co-workers found that intentionally poisoning an Au/TiO_2 catalyst with 5−10 mol % bromide completely shuts down the catalytic activity.[17] We are aware of only one report of CO chemisorption in the literature, using low-temperature pulse chemisorption techniques.[18] Menegazzo and co-workers' measurements on Au/TiO_2 catalysts, which included measurements on a sample of the WGC catalyst, indicated that roughly 3% of the total Au atoms bind CO at temperatures between 150 and 180 K. Their average particle sizes were between 3 and 4 nm, so this is a small fraction of the total surface atoms (around 10%). On the basis of a structural model, the authors concluded that CO bound to about one of every three step-edge sites on the catalyst. Thus, the total number of CO adsorption sites is likely to be only a fraction of the low-coordinated corner and edge atoms.[18]

Recent theoretical work suggests that the primary determinant for catalytic activity on Au nanoparticle catalysts is the availability of low-coordinated gold atoms, which are also likely to be important for oxygen binding and activation [27,45,46] The weak binding and activation of oxygen have long been considered keys to the high catalytic activity of supported Au catalysts, and there is a large body of experimental and theoretical literature suggesting that O_2 adsorption likely occurs on nanoparticle corner or edge sites.[2] This means that O_2, which binds to Au much more weakly than CO, has to compete for similar binding sites. The experimental finding that a substantial fraction of CO binding sites are unoccupied under reaction pressures makes this competition much more plausible.

Because oxygen binding to Au surfaces and nanoparticle catalysts is very weak, it has been extremely difficult to measure. We are aware of only one experimental measurement of the binding constant for O_2 on Au, a kinetic measurement extracted from the oxygen dependence of the catalytic rate during CO oxidation catalysis.[27] This study found the O_2 binding constants for the WGC and MPC catalysts to be similar (both were approximately 35 atm^{-1}, which corresponds to a $\Delta H_{ads} \approx -53$ kJ/mol calculated in the same fashion as above). This value compares very favorably with the high-coverage (weaker) CO binding constants (27 atm^{-1}, or $\Delta H_{ads} \approx -52$ kJ/mol) determined in the current study. The similarity of the high-coverage CO and O_2 binding constants indicates that, even under differential reaction conditions where conversions are low and CO coverage is relatively high and constant, O_2 can effectively compete with CO for the remaining open corner and edge sites. This provides another important explanation for the high activity of Au CO oxidation catalysts: our study shows not only that CO binding sites are available under reaction conditions but also that the similarity between the high-coverage CO and O_2 binding constants under these conditions means that CO and O_2 will bind to the remaining adsorption sites with roughly equal affinity.

Conclusions

CO adsorption on three high surface area Au/TiO_2 catalysts was evaluated with infrared transmission spectroscopy under conditions typically used in CO oxidation catalysis. The three catalysts had essentially the same CO adsorption properties under the pressure range studied (0.05−10 Torr). Binding constants were extracted from the adsorption data using a two-site Langmuir model and a sliding-tangent fit to the Langmuir equation. Both models did a good job of describing the observed coverage dependence of the binding constant. Coverage-dependent heat of adsorption values extracted from the binding constant data were consistent with measurements on planar model systems and under conditions somewhat outside the working conditions of the catalyst.

Comparing the high surface area catalysts with previous measurements on other systems suggests that the CO binding sites are likely to be highly uncoordinated corner and edge atoms. A key result from our studies is that roughly one-quarter of these CO binding sites remain open under CO oxidation catalysis conditions. Further, the high-coverage CO binding constants (or weak CO binding sites) are comparable to O_2 binding constants measured during CO oxidation catalysis. This means that O_2 can effectively compete with CO for the open corner and edge sites, providing an important experimental explanation for the high CO oxidation activity of Au/TiO_2 catalysts.

Acknowledgment. The authors gratefully acknowledge the U.S. National Science Foundation (Grant No. CHE-0449549)

and the Robert A. Welch Foundation (Grant No. W-1552) for financial support of our work.

References and Notes

(1) Bond, G. C.; Louis, C.; Thompson, D. T. *Catalysis by Gold*; Imperial College Press: London, 2006; Vol. 6.

(2) Kung, M. C.; Davis, R. J.; Kung, H. H. *J. Phys. Chem. C* **2007**, *111*, 11767–11775.

(3) Fu, Q.; Saltsburg, H.; Flytzani-Stephanopoulos, M. *Science* **2003**, *301*, 935–938.

(4) Enache, D. I.; Edwards, J. K.; Landon, P.; Solsona-Espriu, B.; Carley, A. F.; Herzing, A. A.; Watanabe, M.; Kiely, C. J.; Knight, D. W.; Hutchings, G. J. *Science* **2006**, *311*, 362–365.

(5) Hughes, M. D.; Xu, Y.-J.; Jenkins, P.; McMorn, P.; Landon, P.; Enache, D. I.; Carley, A. F.; Attard, G. A.; Hutchings, G. J.; King, F.; Stitt, E. H.; Johnston, P.; Griffin, K.; Kiely, C. J. *Nature* **2005**, *437*, 1132–1135.

(6) Corma, A.; Gonzalez-Arellano, C.; Iglesias, M.; Sanchez, F. *Angew. Chem., Int. Ed.* **2007**, *46*, 7820–7822.

(7) Corma, A.; Serna, P. *Science* **2006**, *313*, 332–334.

(8) Boronat, M.; Concepcion, P.; Corma, A.; Gonzalez, S.; Illas, F.; Serna, P. *J. Am. Chem. Soc.* **2007**, *129*, 16230–16237.

(9) Corma, A.; Concepcion, P.; Serna, P. *Angew. Chem., Int. Ed.* **2007**, *46*, 7266–7269.

(10) Christensen, C. H.; Joergensen, B.; Rass-Hansen, J.; Egeblad, K.; Madsen, R.; Klitgaard, S. K.; Hansen, S. M.; Hansen, M. R.; Andersen, H. C.; Riisager, A. *Angew. Chem., Int. Ed.* **2006**, *45*, 4648–4651.

(11) Abild-Pedersen, F.; Andersson, M. P. *Surf. Sci.* **2007**, *601*, 1747–1753.

(12) Mason, S. E.; Grinberg, I.; Rappe, A. M. *Phys. Rev. B: Condens. Matter Mater. Phys.* **2004**, *69*, 161401–161404.

(13) Nieskens Davy, L. S.; Curulla-Ferre, D.; Niemantsverdriet, J. W. *ChemPhysChem* **2006**, *7*, 1075–1080.

(14) Rogal, J.; Reuter, K.; Scheffler, M. *Phys. Rev. B: Condens. Matter Mater. Phys.* **2007**, *75*, 205433.

(15) Zeinalipour-Yazdi, C. D.; Cooksy, A. L.; Efstathiou, A. M. *Surf. Sci.* **2008**, *602*, 1858–1862.

(16) Ponec, V.; Bond, G. C. Eds. *Catalysis by Metals and Alloys*; Elsevier: Amsterdam, 1995; Vol. 95.

(17) Oxford, S. M.; Henao, J. D.; Yang, J. H.; Kung, M. C.; Kung, H. H. *Appl. Catal., A* **2008**, *339*, 180–186.

(18) Menegazzo, F.; Manzoli, M.; Chiorino, A.; Boccuzzi, F.; Tabakova, T.; Signoretto, M.; Pinna, F.; Pernicone, N. *J. Catal.* **2006**, *237*, 431–434.

(19) Meier, D. C.; Goodman, D. W. *J. Am. Chem. Soc.* **2004**, *126*, 1892–1899.

(20) Zhao, Z.; Diemant, T.; Rosenthal, D.; Christmann, K.; Bansmann, J.; Rauscher, H.; Behm, R. J. *Surf. Sci.* **2006**, *600*, 4992–5003.

(21) Diemant, T.; Hartmann, H.; Bansmann, J.; Behm, R. J. *J. Catal.* **2007**, *252*, 171–177.

(22) Lemire, C.; Meyer, R.; Shaikhutdinov, S. K.; Freund, H. J. *Surf. Sci.* **2004**, *552*, 27–34.

(23) Yim, W.-L.; Nowitzki, T.; Necke, M.; Schnars, H.; Nickut, P.; Biener, J.; Biener, M. M.; Zielasek, V.; Al-Shamery, K.; Kluener, T.; Baeumer, M. *:J. Phys. Chem. C* **2007**, *111*, 445–451.

(24) Meier, D. C.; Bukhtiyarov, V.; Goodman, D. W. *J. Phys. Chem. B* **2003**, *107*, 12668–12671.

(25) Kim, J.; Samano, E.; Koel, B. E. *J. Phys. Chem. B* **2006**, *110*, 17512–17517.

(26) Derrouiche, S.; Gravejat, P.; Bianchi, D. *J. Am. Chem. Soc.* **2004**, *126*, 13010–13015.

(27) Long, C. G.; Gilbertson, J. D.; Vijayaraghavan, G.; Stevenson, K. J.; Pursell, C. J.; Chandler, B. D. *J. Am. Chem. Soc.* **2008**, *130*, 10103–10115.

(28) Korkosz, R. J.; Gilbertson, J. D.; Prasifka, K. S.; Chandler, B. D. *Catal. Today* **2007**, *122*, 370–377.

(29) CO adsorption on TiO_2, which appeared as a peak near 2050 m^{-1} (wavenumber), was only observed at much lower temperatures, ca. below 253 K.

(30) Hakkinen, H.; Abbet, S.; Sanchez, A.; Heiz, U.; Landman, U. *Angew. Chem., Int. Ed.* **2003**, *42*, 1297–1300.

(31) Dumas, P.; Tobin, R. G.; Richards, P. L. *Surf. Sci.* **1986**, *171*, 579–599.

(32) Bradshaw, A. M.; Pritchard, J. *Proc. R. Soc. A* **1970**, *316*, 169–183.

(33) France, J.; Hollins, P. *J. Electron Spectrosc. Relat. Phenom.* **1993**, *64−65*, 251–258.

(34) Chen, M.; Cai, Y.; Yan, Z.; Goodman, D. W. *J. Am. Chem. Soc.* **2006**, *128*, 6341–6346.

(35) Spiewak, B. E.; Dumesic, J. A. *Thermochim. Acta* **1998**, *312*, 95–104.

(36) Guerrero-Ruiz, A.; Maroto-Valiente, A.; Cerro-Alarcon, M.; Bachiller-Baeza, B.; Rodriguez-Ramos, I. *Top. Catal.* **2002**, *19*, 303–311.

(37) Phillips, J. *J. Therm. Anal.* **1997**, *49*, 541–552.

(38) Podkolzin, S. G.; Shen, J.; De Pablo, J. J.; Dumesic, J. A. *J. Phys. Chem. B* **2000**, *104*, 4169–4180.

(39) Shen, J.; Hill, J. M.; Watwe, R. M.; Podkolzin, S. G.; Dumesic, J. A. *Catal. Lett.* **1999**, *60*, 1–9.

(40) Xia, X.; Naumann d'Alnoncourt, R.; Muhler, M. *:J. Therm. Anal. Calorim.* **2008**, *91*, 167–172.

(41) Roze, E.; Gravejat, P.; Quinet, E.; Rousset, J. L.; Bianchi, D. *J. Phys. Chem. C* **2009**, *113*, 1037–1045.

(42) Manzoli, M.; Chiorino, A.; Boccuzzi, F. *Surf. Sci.* **2003**, *532−535*, 377–382.

(43) As a reviewer pointed out, the CO coverage under reaction conditions is more complicated. In a working reactor, CO coverage will depend on the conversion at any given time and will vary throughout the reactor bed. We, therefore, present the arguments regarding CO and O_2 competition in the context of the limiting case of differential reaction conditions. Under these conditions, conversions are low (<2%) and reactant pressures are essentially constant throughout the reactor bed. CO coverages are, therefore, constant and approximately equal to the inlet composition of the feed. This represents the "worst-case scenario" for O_2 competition because the number of available binding sites is minimized. At higher conversions, the CO partial pressure (and, therefore, coverage) drops throughout the reactor, freeing up even more sites for O_2 binding and activation. So, as long as the CO pressure is near or below 1% CO, the data indicate that a substantial fraction of the CO binding sites will be available for O_2 binding.

(44) Falsig, H.; Hvolboek, B.; Kristensen, I. S.; Jiang, T.; Bligaard, T.; Christensen, C. H.; Noerskov, J. K. *Angew. Chem., Int. Ed.* **2008**, *47*, 4835–4839.

(45) Lopez, N.; Janssens, T. V. W.; Clausen, B. S.; Xu, Y.; Mavrikakis, M.; Bligaard, T.; Norskov, J. K. *J. Catal.* **2004**, *223*, 232–235.

(46) Xu, Y.; Mavrikakis, M. *J. Phys. Chem. B* **2003**, *107*, 9298–9307.

JP902553N